Geological Evolution of Venus: Rises, Plains, Plumes, and Plateaus

Roger J. Phillips* and Vicki L. Hansen

Crustal plateaus and volcanic rises, major physiographic features on Venus, both formed over mantle plumes. Crustal plateaus were produced by large degrees of plume melting beneath thin lithosphere. The oldest tectonic features in crustal plateaus are ribbon-like troughs indicating early uplift and tensile stretching; their shallow depths suggest that surface temperature there was higher in the past. Widespread volcanic plains, derived from the broad upwellings of internally heated mantle convection, were continually erupted during the time of crustal plateau formation. Discrete volcanic rises, younger than crustal plateaus, formed over a thicker lithosphere, with less plume partial melting. The presence of only one transitional form indicates that the lithosphere thickened rapidly. Thermal and magmatic models show that the formation of these major features can be tied to an expected change in mantle convective style about 1 billion years ago.

The recognition of the significance of just two major terrestrial tectonic features in the oceans—midocean ridges and trenches—established the paradigm of seafloor spreading and subduction. This recognition in turn provided the kinematic foundation for plate tectonics, an elegant theory providing a coherent framework for understanding how Earth's broad geomorphic features—including volcanic chains and continental mountain belts—relate to heat escape and interior processes. Similarly, understanding the differences in the formation of two major features on Venus—crustal plateaus and volcanic rises—is key for understanding the geological evolution of that planet over the last billion years. In this article, we examine the geology of these features and present a model for their formation and of the thermal evolution of the lithosphere (*1*) of Venus. We suggest that the features both formed as a result of the interaction with the lithosphere of mantle plumes rising from the core-mantle boundary.

Volcanic plains, volcanic rises, and crustal plateaus make up more than 80% of the surface area of Venus. Plains are dominant (~65 to 70% by area), reside at low elevations, and show minor, but broadly distributed deformation. Nine volcanic rises (*2*) and five crustal plateaus are similar in planform shape and size, but differ in topography, gravity, and surface geology (*3, 4*). Volcanic rises are dome-like regions (1000- to 2400-km diameters) and contain rift zones, lava flows, and major volcanic edifices (*5*). Their large gravity anomalies and relatively low crater densities suggest that they are young features (*6–8*), largely supported thermally by their buoyant plume source. Crustal plateaus are steep-sided, flat-topped, quasi-circular regions that host most of the planet's tesserae (complexly deformed crust). Plateaus have small gravity anomalies consistent with isostatic compensation by a thick crust (*6, 9–11*). As a class, plateaus are older than rises on the basis of crater densities (*12*).

The Origin of Crustal Plateaus

The basis for suggesting that rises and plateaus can be explained by mantle plumes and reflect the systematic cooling of Venus is a recent interpretation of the structural geology of crustal plateau tesserae indicat-

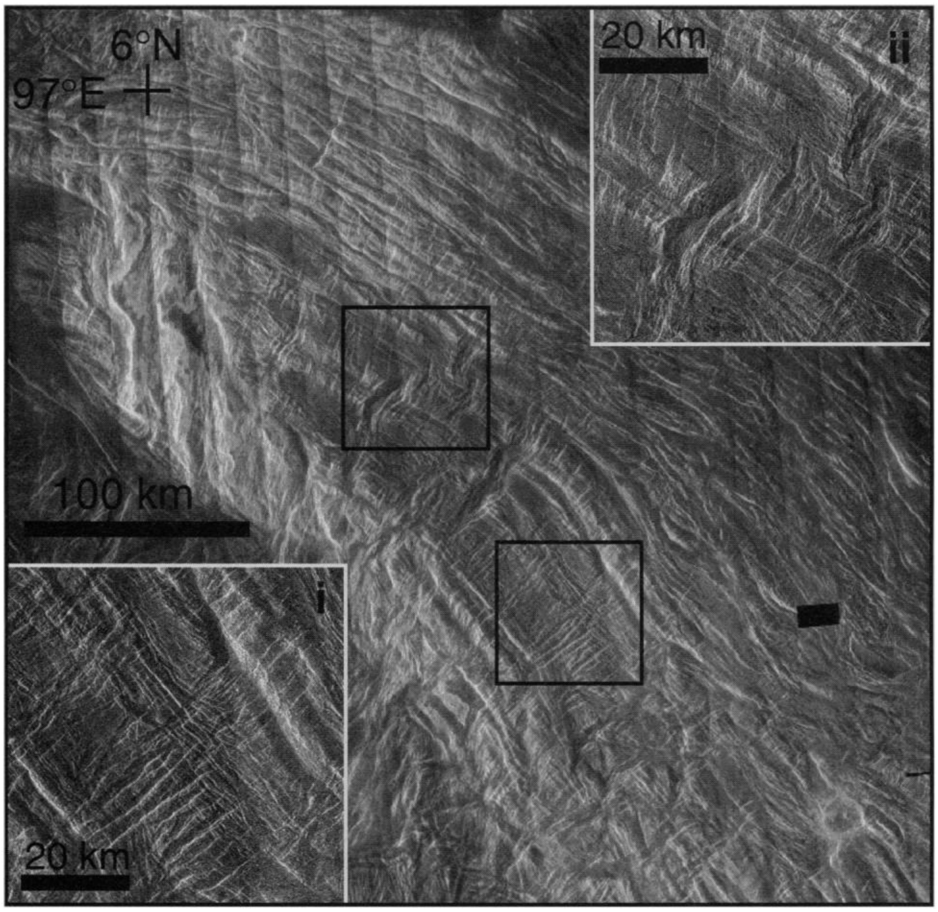

Fig. 1. Crests of NW-trending folds are cut by NE-trending lens-shaped graben. Ribbons parallel graben although they differ in structural style and geometry (insets). Ribbons (**i**) are marked by bright and dark paired lineaments >50 to 100 km long; these lineaments define alternating, flat-topped ridges and narrow, steep-sided, flat-bottomed troughs. In contrast, graben (**ii**) host numerous accommodation structures, they have aspect ratios of 3 to 4 rather than >50, their walls are sloped inward ~60°, and they are lens-shaped with the widest part of the graben superimposed on fold crests.

R. J. Phillips is in the Department of Earth and Planetary Sciences, Washington University, Campus Box 1169, One Brookings Drive, St. Louis, MO 63130, USA. V. L. Hansen is in the Department of Geological Sciences, Southern Methodist University, Dallas, TX 75275, USA.

*To whom correspondence should be addressed.

ing that the earliest preserved deformation is extensional (*13*, *14*). This contradicts a widely accepted model for the formation of crustal plateaus by convective mantle downwelling and secondary crustal thickening (*15–17*). The downwelling model was supported by an interpretation of radar images that the oldest preserved deformational features in these plateaus are contractional, not extensional, in nature (*18–20*). Geodynamical models of crustal plateau formation by convective downwelling predict that the high areas of a plateau should have first undergone contraction (*21*, *22*), whereas a buoyancy brought about by plumes should initially extend the surface (*21*, *23*).

A key area for understanding the sequence of deformation on crustal plateaus is the northeastern part of the crustal plateau Ovda Regio. Here, northeast-trending graben do indeed cut the crests of northwest-trending folds, indicating that surface contraction predated extension (Fig. 1). Close examination, however, reveals a third structural feature. "Ribbons" [named for their long linear character and high length versus width (*13*)] parallel the late graben yet differ in structural style. Ribbon structures comprise a fabric of steep-sided, alternating ridges and troughs. These structures have been recognized as distinct from the late graben [for example, "steep troughs" (*18*) or "narrow troughs" (*17*, *24*)], but it was typically assumed that graben-fold temporal relations applied to ribbons as well. In addition to their difference in structural style, ribbons are much more widely distributed across individual crustal plateaus, unlike the graben. Ribbons occur within each of the crustal plateaus except Phoebe Regio (*4*, *25*).

Radar analysis of ribbon structures indicates that typical ribbons are steep-sided (>85°), flat-bottomed, shallow (<0.4 km) troughs with V-shaped lateral terminations (Fig. 2) indicating that they result from opening of tensile fractures in a thin strong brittle layer above a weaker ductile substrate, like a chocolate layer atop a caramel bar (*26*). Locally ribbons are bounded by steep extensional shear fractures, representing dominantly brittle deformation of a strong layer above a weak substrate. The typical spacing between ribbons of ~1 to 2 km and their morphology are consistent with the inference that ribbons formed from extension of a thin (<1 km) brittle layer of the crust (*14*). The ribbon floors then mark the depth to a brittle-ductile transition (BDT). These depths are <0.5 km for tensile-fracture ribbons and 0.6 to 1.2 km for shear-fracture ribbons (*13*). In contrast, the typical wavelength of crustal plateau folds of ~15 km implies that the depth to the BDT when folds formed was ~6 km (*27*). Because ribbons and folds are found together, it is most reasonable that the ribbons, which reflect a shallow depth of the BDT, formed before the folds. If the ribbons formed after the folds, the folds would not be supported by the shallow BDT, and they would have disappeared by viscous relaxation. However, if ribbons formed first and folds formed later as the depth to the BDT increased with time, the observed geometric characteristics of both types of structures could be accommodated. These mechanical considerations are consistent with geometric analyses that require ribbons to predate folds (*14*). The late graben, which formed after the folds, likely reflect a still deeper depth to crustal BDT, as evidenced by their spacing of >25 km. The complete deformational sequence suggests progressive cooling of an individual crustal plateau with time, and is consistent with plateau formation by an upwelling plume, magmatic injection into the crust, solidification, and subsequent cooling of the rock mass.

The idea that crustal plateaus are genetically related to plumes was raised before (*28*, *29*), in which a volcanic rise evolved into a crustal plateau by continued subsurface addition of magmatic material to the crust overlying the plume. This model was criticized because crustal plateaus do not show any remnants of an earlier volcanic rise stage, particularly large shield volcanoes (*17–19*). The hypothesis also holds that crustal plateaus as a class are younger than volcanic rises, in conflict with impact crater densities.

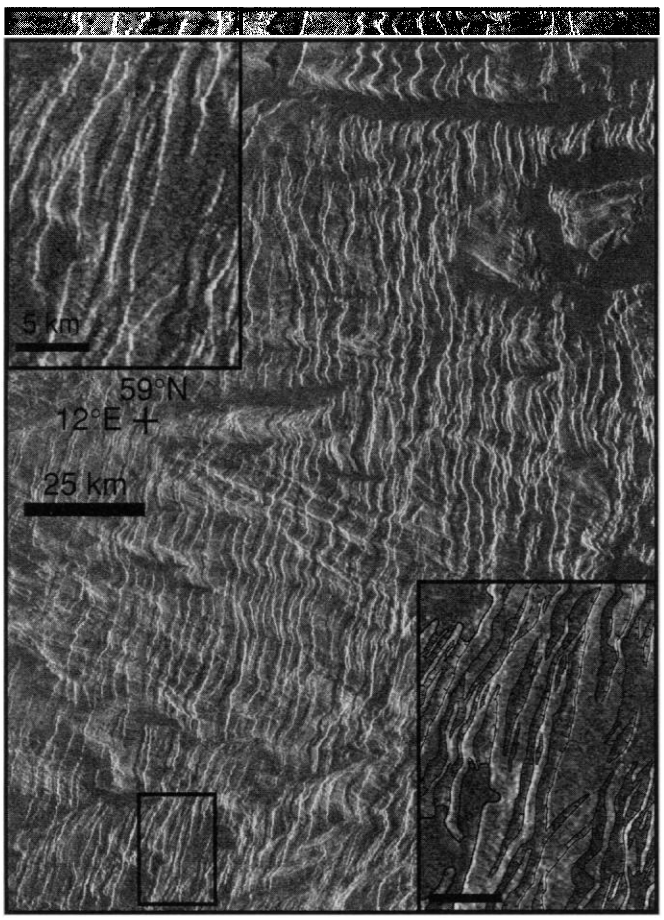

Fig. 2. North-trending ribbons (paired dark and light lineaments) track across E-trending fold crests in Fortuna Tessera. The apparent deflection of the ribbons across the crest of the folds toward the radar (left) is the result of radar foreshortening, an imaging artifact; parallelism of opposite ribbon trough slopes across the folds indicates that the slopes are very steep, >85° (*14*). Insets show an enlargement of the region in the box; ribbon troughs are marked by tic marks, ridges are between the troughs. Note V-shaped joining of walls on opposite sides of the troughs.

Temporal Constraints

Any plausible geological model of Venus must satisfy available age constraints, which are based primarily on counts and sizes of impact craters. The average surface age of Venus is estimated to be 750 million years ago (Ma) (*30*). Tesserae, which make up most of the crustal plateaus, have an average age of 900 ± 220 Ma (*31*). Volcanic rises have large gravity anomalies, implying that they are dynamically supported at depth today and thus are young. Additionally, features associated with volcanic rises (for example, large volcanoes) are younger than the global average surface age by up to a factor of 4 (*8*). In some cases, however, the average surface age of a rise is not young because much of the surface is composed of uplifted old plains (for example, Beta Regio).

The volcanic plains of Venus are roughly divisible into four geomorphic units (*32*,

33) that overlap in time and span a total age range of more than 1000 to 600 Ma (30). The two youngest plains units are spatially associated with chasmata (rifts) and centers of young constructional volcanism (32). More generally, the two youngest plains units can be combined into a single unit of "young plains" (33% of total plains area) with an average age of 675 ± 50 Ma, and the two other units lumped into "old plains" (34) with an average age of 975 ± 50 Ma. This division is visually obvious on a global map of crater density.

Global Geological Model

The geological and temporal relations summarized above can be explained if crustal plateaus and volcanic rises both formed above plumes, but at distinctly different times, with different lithospheric thicknesses, and hence within different magmatic environments because of the depth of melting (Fig. 3). We suggest that plateaus formed early when the lithosphere was thin (mobile or thin-lid regime) during a time of prolific magmatism; rises formed later in thick lithosphere (stagnant- or thick-lid regime) when magmatic activity was relatively low. The transition in magmatic rates could have been brought about by a change in convective style in the mantle attributable simply to secular cooling of the planet. We suggest that in addition to centralized crustal plateau magmatism, the thin-lid regime also permitted regional eruptions of volcanic flows to form most of the existing plains. As focused plumes rising from the core-mantle boundary were undergoing extensive partial melting in the upper mantle to form crustal plateaus, internally heated convection in the mantle caused diffuse upward motion of large volumes of mantle (35), triggering spatially widespread partial melting and plains volcanism as a result of pressure-release melting under a thin lithosphere.

During Venus' thin-lid period, a process akin to plate tectonics may have developed, although delamination of the uppermost mantle beneath the crust could instead have served to recycle cold material to the deeper mantle (Fig. 3). During plume upwelling in this period, the crust heats rapidly by injection of magma; it uplifts, thickens, then cools and subsides. Ribbon fabrics would be expected to form first during uplift, when the BDT was shallow and tensile stresses were high. Gravitational sliding and limited contraction along the plateau margins would have thickened the crust in these regions. As the hot, thickened, crust eventually cooled; local slumping of the previously inflated crust led to local, limited, disorganized shortening at the surface, and the BDT deepened. Eventually, a plateau is left with thick isostatically compensated crust, which is unstable and so, with time, collapses into the surrounding lowlands. This model implies that the existing crustal plateaus formed relatively late in the thin lithospheric lid phase and were captured and preserved within the thickening lithosphere. We propose that earlier formed crustal plateaus are locally preserved as large tessera inliers (3, 4), many of which host ribbon terrain structures (17, 36). After the transition to a thick lid, large amounts of melting in the mantle is no longer possible, so volcanic rises, rather than crustal plateaus, form on the stronger, thicker lithosphere. Lacking, a crustal root, volcanic rises must be supported dynamically by plumes and will collapse as the plume ebbs. The stress state of the lithosphere also changes, so that rifts, and coronae (37) associated with them, become the prevalent tectonic style. Plains volcanism continues, but at a greatly reduced rate (33).

Our model and age estimates of the Venus crust provide a prediction of how rapidly the lithosphere thickened. We place the switch from mobile (thin) to stagnant (thick) lid at 700 Ma under the supposition that some of the young plains formed during the transition period from thin to thick lid when the stress state in the lithosphere fundamentally changed and magmatism was declining. The absence of extensive plains younger than 600 Ma might suggest that formation of plains ceased quickly, although we do not know the true age range of plains. The limited number of embayed craters on the plains may imply that volcanism tailed off rather quickly, perhaps over 100 My (12), but this evidence is weak. Another argument is that if the lithosphere thickened gradually, then, according to our hypothesis, we should observe a number of structures that are transitional between crustal plateaus and volcanic rises, yet we find only one candidate feature: Phoebe Regio is characterized by a complex pattern of extensional graben and lack of ribbons (4, 13).

A change in mantle convective style at ~700 Ma could have led to a rapid increase in the thickness of the lithosphere. Because the viscosity contrast between the surface and the interior of a terrestrial planet is large, a thick, stagnant lithospheric lid should form (38). An exception to this scenario occurs if, like the Earth, a planet is able to recycle a portion of its strong lithosphere because it can be broken (that is, a thin- or mobile-lid regime; Earth's version of this is plate tectonics). As a planet cools and radiogenic heat production wanes, convection in the mantle slows and the induced stress on the overlying lithosphere diminishes. Heat flux into the lithosphere also decreases, so the lithosphere cools and strengthens and becomes harder to break. Eventually, recycling comes to an end, and

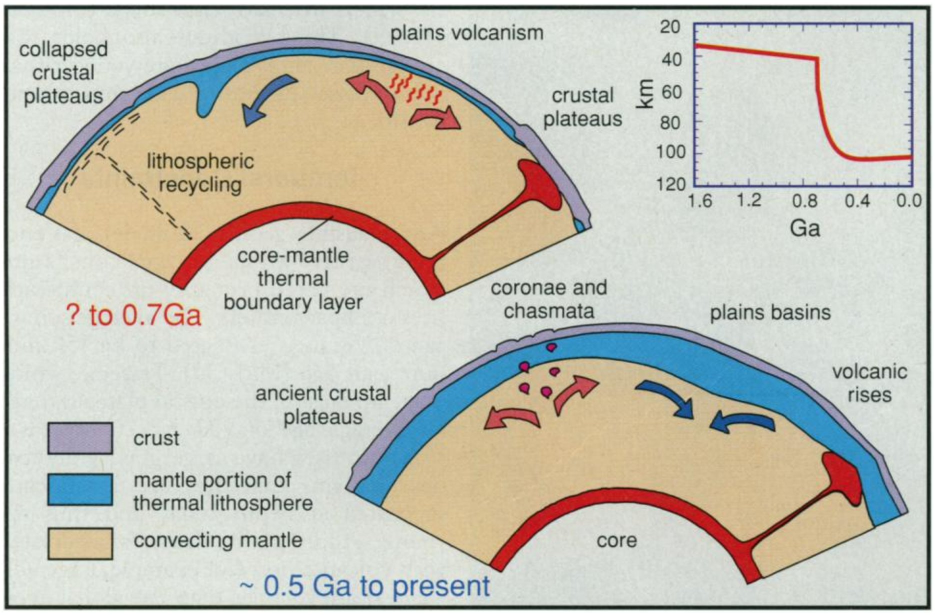

Fig. 3. Cartoon illustrating the major tectonic and magmatic processes operating in the thin (mobile)-lid regime (>0.7 Ga) and in the thick (stagnant)-lid regime (~0.5 Ga to present). The boxed inset shows thermal lithosphere thickness (km) versus age as calculated from a thermal model. In the thin-lid era, lithospheric recycling was associated with mantle downwellings whose surface expression included ridge belts. In the thick-lid era, lithospheric extension over a heating mantle produces corona chains and chasmata, which mark broad diffusive mantle upwellings; the topographic basins of the plains reflect mantle downwellings (3).

the lithosphere rapidly thickens and becomes stagnant. This switch from a mobile to stagnant lithospheric lid is a natural consequence of terrestrial planetary evolution. The question is whether a stagnant lid is stable or whether it can collapse into a vigorous but transient episode of lithospheric recycling (subduction) followed by reformation of a stagnant lid (39).

Some numerical models of mantle convection show repeated episodes of stagnant lid collapse, each followed rapidly by a short-lived episode of lithospheric subduction (39). Similarly, one model of the evolution of Venus (16, 40), based on inferences from the cratering record (41), is that a transient subduction event led to widespread volcanism and rapid global resurfacing of the planet. However, the cratering record provides information only into the period of resurfacing decline and cannot be used to distinguish between a punctuated resurfacing event and the end of a sustained period of resurfacing. We suggested above that the major plains units span about 400 My and extend back in time from the transition from a thin to a thick lid. We cannot say whether there were transient events before this period, or whether in the future the present thick lid will collapse. Additionally, some models (16, 40) predict that the present lithospheric thickness is about 300 km; this value is sufficiently thick to prohibit magmatic activity, contrary to observation (33).

Herrick (42) proposed that a mobile-lid phase ended on Venus in the last billion years. His model differs from ours in two ways. First, he suggested that tesserae record the mobile-lid deformation and are globally pervasive, whereas we argue that most tesserae are associated with crustal plateaus or remnants of them, as supported by geologic mapping (25). Secondly, Herrick argued that the volcanic plains were rapidly emplaced at the end of the mobile-lid era after all tesserae had formed, while we suggest that plains deposition was an ongoing process during the thin-lid era. The western margin of Tellus Regio preserves ~1000 km of a deformation front in which crustal plateau tesserae grade into preexisting plains units, so tesserae are not everywhere older than plains, as has been suggested (12, 17, 43). Elsewhere, many of the youngest volcanic plains units onlap tesserae at crustal plateau boundaries. Thus in most cases the youngest portion of volcanic plains formed locally after adjacent crustal plateaus, although we argue that both types formed broadly at the same time.

During the formation of the voluminous plains, outgassing of volatiles should have enhanced the atmospheric greenhouse of Venus and thereby increased the surface temperature. In turn, higher surface temperatures would have decreased the heat flux from the lithosphere and increased interior temperatures and the amount of melting. Enhanced magmatism would then provide more volatiles to the atmosphere. Such a feedback mechanism would imply that the interior and climatic processes of Venus were tightly coupled during the thin-lid phase. Surface temperatures could have approached 1000 K (44) during thin-lid time.

Computational Models

To further test the geodynamical plausibility of our interpretations, we considered results from a numerical simulation of the thermal evolution of Venus and of the generation of magmas in the mantle. We computed a thermal evolution using a one-dimensional parameterized convection approach (45, 46). The thermal structure of the mantle and of plumes rising off the core-mantle boundary, along with minimum depth of melting controlled by lithosphere thickness, determine melting behavior. Temperatures in the convecting mantle and in the core are determined by using the conservation of thermal energy along with a relationship between the Nusselt number and the thermal Rayleigh number (47). The parameters in the Nusselt number–Rayleigh number relationship are changed commencing at 700 Ma; the Nusselt number decreases and the lithosphere thickens in response. In thin-lid convection, heat transfer is dominated by cooling of the mantle with recycled lithosphere; the characteristic conversion time to thick-lid behavior of the Nusselt number–Rayleigh number relationship is equated to the thermal assimilation time of the subducted prechange lithosphere. The time scale of lithospheric thickening is controlled by the thermal equilibrium time of the new lithosphere modeled as a conductive slab. The results of a specific thermal model calculation yield time-dependent estimates of mantle and core temperatures, lithospheric thickness, and heat flux, providing the basic information for partial melt calculations. We included the effects of an enhanced greenhouse by using a 1000 K surface temperature during thin-lid time and then decreasing it to 740 K during the 50 My after a thick lid started to form.

Plume temperature was obtained from the core-mantle thermal boundary layer, weighted 75% and 25% between the solution temperatures obtained at the bottom and top of the boundary layer, respectively (48). To obtain a temperature for melting calculations near the top of the mantle, the plume was cooled adiabatically and also assumed to lose diffusively a fraction, f_p, of its initial temperature. The temperature for melting of diffuse mantle upwellings to produce plains volcanism is the upper mantle temperature possibly increased by a small amount ΔT_p. The two temperatures (plumes, plains) obtained are converted to potential temperatures by adiabatically reducing them to their zero pressure values because potential temperature is used in determining melt fraction. We assume that the lithosphere (thickness, H) was thermally eroded and stretched so that the effective depth for melting is $H\Delta L_{plu}$ for plumes and $H\Delta L_{upw}$ for upwellings. These values establish minimum melting depths. Given potential temperature and lithostatic pressure at the base of the eroded and stretched lithosphere, partial melt fraction, or equivalent melt column height, can be calculated for both plumes and plains (49). The numerical solution used as input for a partial melting calculation is called a "computational thermal model" (CTM), and the result of a partial melting calculation is referred to as a "computational melting model" (CMM).

There are a relatively large number of free parameters in the CTM, but Table 1

Table 1. Constraints for thermal and magmatic modeling. CP, crustal plateau; VR, volcanic rise; Ga, billions of years ago.

Observable	Interpretation or estimation	Implication
Ribbons	CP earliest strain event extensional	Plume origin for CPs
Gravity	CP have thick crustal roots VR dynamically supported	Magmatism played a stronger role in CP formation
Heat flow	36 to 55 mW m^{-2}	Present lithosphere thickness is Earth-like
Phoebe Regio	Only candidate for transition from CP to VR	Lithosphere thickened quickly
	Global geological model	
Plumes	First created CP then VR	Melting in plumes declined at 0.6 to 0.7 Ga
Plains	Plains generation extensive before 0.7 Ga; meager during present thick-lid era	Melting in mantle declined at 0.6 to 0.7 Ga

shows that the combination of geological and geophysical constraints, plus our global geological model, provide a number of guidelines for selecting parameter values (*50*). It was not our intent to use the constraints in Table 1 to estimate parameters of the CTM; rather, we sought geologically and geophysically plausible sets of parameters to satisfy the constraints listed. Thus the CTM was tuned to the geological and geophysical constraints described above. Subsequently we investigated other predictive properties of the CTM for the parameter values adopted, including the crustal plateau formation rate, the plains emplacement rate, and the behavior with time of the depth to the BDT in crustal plateaus. Because plains, crustal plateaus, and volcanic rises areally represent most of Venus, our results have global implications.

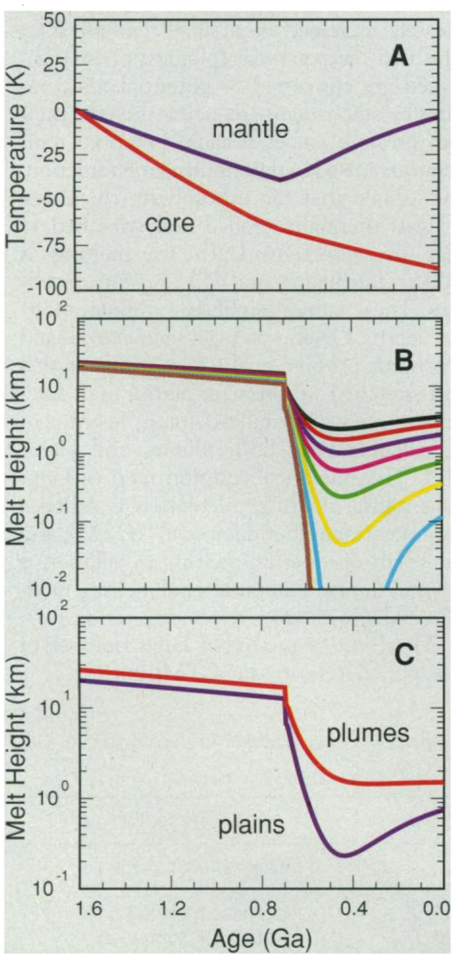

Fig. 4. (**A**) CTM-computed temperatures as a function of age in the uppermost convecting mantle (blue) and at the top of the iron core (red) referenced to their values at 1.6 Ga. (**B**) A suite of CMM models for the height of plains-forming melt column as a function of lithospheric penetration, ΔL_{upw}. Curves from top to bottom are a range in ΔL_{upw} from 0.70 to 1.05 in increments of 0.05. (**C**) Melting curves for nominal model (*51*) of plains (blue) and plumes (red).

The nominal computational model (*51*) satisfies the constraints of Table 1, including a present-day surface heat flow of 44 mW m^{-2}. At the convective switch, the lithosphere thickens from ~40 km to over 100 km over ~200 My (Fig. 3). At the same time the upper mantle temperature increases while the rate of cooling of the outer core decreases (Fig. 4A). This evolution implies that the partial melting histories of plains and plumes will be quite different. A suite of models varying the lithosphere erosion-stretching parameter, $H\Delta L_{upw}$, shows that a basic feature of plains generation is, after the switch, a decrease in melt generation due to the rapidly thickening lithosphere followed by a partial recovery due to the increasing temperature of the upper mantle (Fig. 4B). Depending on the choice of $H\Delta L_{upw}$, partial melting can be completely eliminated or decreased by only a moderate amount (*52*). The nominal model has a modest recovery in plains volcanism, consistent with the imposed constraints of Table 1 (Fig. 4C). Also calculated is a plume curve (Fig. 4C), where melt generation decreases to a relatively constant value; here the increase in lithospheric thickness dominates melt behavior because the core cooling rate, which controls plume temperature, changes only modestly. The decrease in melt generation is nearly a factor of 20, consistent with the generation of volcanic rises, not crustal plateaus, after the switch.

Our calculations (Fig. 4) indicate the potential for pressure-release partial melting when hot mantle material is brought near the base of the lithosphere, but they do not provide rates of melt generation. The plume rate can be estimated from the amount of model-calculated heat supplied by the core to the core-mantle thermal boundary layer, where plumes originate (*53*). In the billion years preceding the switch, the CMM predicts (CTM parameters were not tuned for this particular result) that enough partial melt by volume is generated to produce about 13 features the size of the crustal plateau Tellus Regio (*54*). This amount would account for the five observed crustal plateaus in about the same interval of geological history. Given this rate, and the possibility of at most one observed geologic structure, Phoebe Regio, that could be intermediate between crustal plateaus and volcanic rises, the expected thickening time of the lithosphere is a few hundred million years. This result supports our hypothesis that the lithosphere must have thickened rapidly compared to that expected from the slow secular cooling brought about by a loss of heat-producing parent isotopes (without a corresponding change in convective style). Because the CTM shows that a change in mantle convective style has only a small effect on core cooling, it also follows that plume-derived crustal plateaus could not have all formed during a single punctuated event of subduction (*16*).

Broad upwellings associated with mantle convection should produce widespread, active plains volcanism in the thin-lid era. According to the CMM, this process produces a volume partial melt fraction, φ, of 21% at 1.7 Ga decreasing to 17% at 0.7 Ga. The volume per unit area of melt produced for plains emplacement is the product of the diffuse upwelling velocity, v_u, and φ. If v_u is even as small as 0.1% of the convection boundary layer velocities obtained from the CTM, then vertical plains emplacement rates vary from 10 km per billion years at 1.7 Ga to 5 km per billion years at 0.7 Ga. Higher velocities may imply significant crustal recycling, but the major point is that a plausible set of model parameters predicts that volcanic plains emplacement was a dominant, ongoing process during thin-lid time and not a punctuated event. Given the rarity of crustal plateau genesis, then, as observed, exposed volcanic plains should be almost everywhere younger than crustal plateaus. This does not, however, imply that plains emplacement was a single event that followed all crustal plateau formation, contrary to other viewpoints (*12, 17, 43*).

Ribbon Formation

The development of tensile ribbons places severe constraints on the thermal environment of crustal plateaus. The shallow crust had to be free of preexisting faults and throughgoing fractures, which would have been reactivated at stresses lower than the tensile strength of the crust (*55, 56*). Vast areas in crustal plateaus must have been mechanically suited to ribbon formation. Either a plateau crust was not previously deformed, or it had been annealed by solid-state creep or magma injection. Furthermore, the crust must have been hot enough, long enough, to sustain tensile failure at shallow depths. The magmatic origin of crustal plateaus may provide the proper environment; injection of magma into fractures could have created a mechanically homogeneous environment in which to form ribbons. At a surface temperature of 740 K, model calculations (*57*) show that the BDT would rapidly deepen as the crust cooled; shear failure would be expected at a depth of 1 km after only about 20,000 years (*58*). At a surface temperature of 1000 K, this time increases by a factor of 15, and the shear fracture ribbons could be expected to have formed within 1 My. This time approaches the duration of large terrestrial flood basalt events, which have been linked to substantial partial melting in mantle plume heads (59). The most important message from the ribbons may be that the climate and internal history of Venus were strongly coupled throughout much of its history.

REFERENCES AND NOTES

1. Lithosphere is defined as the strong outer shell of a terrestrial planet that transports heat to the surface by conduction.
2. S. E. Smrekar, W. S. Kiefer, E. R. Stofan, in *Venus II*, S. W. Bougher, D. M. Hunten, R. J. Phillips, Eds. (Univ. of Arizona Press, Tucson, 1997), pp. 845–878.
3. R. J. Phillips and V. L. Hansen, *Annu. Rev. Earth Planet. Sci.* **22**, 597 (1994).
4. V. L. Hansen, J. J. Willis, W. B. Banerdt, in (*2*), pp. 797–844.
5. E. R. Stofan *et al.*, *Geol. Soc. Am. Bull.* **101**, 143 (1989); D. A. Senske, G. G. Schaber, E. R. Stofan, *J. Geophys. Res.* **97**, 13395 (1992).
6. S. E. Smrekar and R. J. Phillips, *Earth Planet. Sci. Lett.* **107**, 582 (1991).
7. R. E. Grimm and R. J. Phillips, *J. Geophys. Res.* **97**, 16035 (1992); S. E. Smrekar, *Icarus* **112**, 2 (1994).
8. N. Namiki and S. C. Solomon, *Science* **265**, 929 (1994); M. Price and J. Suppe, *Nature* **372**, 756 (1994); R. J. Phillips and N. R. Izenberg, *Geophys. Res. Lett.* **22**, 1517 (1995); M. H. Price, G. Watson, J. Suppe, C. Brankman, *J. Geophys. Res.* **101**, 4657 (1996).
9. R. R. Herrick and R. J. Phillips, *J. Geophys. Res.* **97**, 16017 (1992).
10. R. E. Grimm, *Icarus* **112**, 89 (1994); M. Simons, S. C. Solomon, B. H. Hager, *Geophys. J. Int.* **131**, 24 (1997).
11. R. E. Grimm and P. C. Hess, in (*2*), pp.1205–1244.
12. A. T. Basilevsky, J. W. Head, G. G. Schaber, R. G. Strom, in (*2*), pp.1047–1084.
13. V. L. Hansen and J. J. Willis, *Icarus* **123**, 296 (1996).
14. ———, *ibid.*, in press.
15. S. C. Solomon, *Phys. Today* **46**, 48 (1993).
16. D. L. Turcotte, *J. Geophys. Res.* **98**, 17061 (1993).
17. M. A. Ivanov and J. W. Head, *ibid.* **101**, 14861 (1996).
18. D. L. Bindschadler G. Schubert, W. M. Kaula, *ibid.* **97**, 13495 (1992).
19. D. L. Bindschadler A. DeCharon, K. K. Beratan, S. E. Smrekar, J. W. Head, *ibid.*, p. 13563.
20. D. L. Bindschadler, *Rev. Geophys. (Suppl.)* **33**, 459 (1995).
21. D. L. Bindschadler and E. M. Parmentier, *J. Geophys. Res.* **95**, 2132 (1990).
22. A. Lenardic, W. M. Kaula, D. L. Bindschadler, *Geophys. Res. Lett.* **18**, 2209 (1991).
23. R. J Phillips, *J. Geophys. Res.* **95** 1301 (1990).
24. J. W. Head, *Lunar Planet Sci.* **XXVI**, 579 (1995).
25. R. R. Ghent and V. L. Hansen, *ibid.* **XXVIII**, 409 (1997).
26. The type ribbons are located in southeastern Fortuna Tessera (*14*).
27. C. D. Brown and R. E. Grimm, *Earth Planet. Sci. Lett.* **147**, 1 (1997).
28. R. R. Herrick and R. J. Phillips, *Geophys. Res. Lett.* **17**, 2129 (1990).
29. R. J. Phillips, R. E. Grimm, M. C. Malin, *Science* **252**, 651 (1991).
30. W. B. McKinnon, K. J. Zahnle, B. I. Ivanov, H. J. Melosh, in (*2*) pp. 969–1014. Age estimates of a specific geologic unit are obtained by scaling its crater density to the global mean crater density.
31. Only craters with diameters ≥32 km are counted to avoid a potential observational bias [M. A. Ivanov and A. T. Basilevsky, *Geophys. Res. Lett.* **20**, 2579 (1993)]. This estimate averages, across all of the tesserae, the oldest surviving crater on each tessera (the "retention age"). This age is less than the average formation age of the tesserae themselves. The errors used here and elsewhere are 1σ values based on counting statistics and do not take into account the uncertainty in the 750 Ma mean age value (*30*).
32. M. Price, *Proc. Lunar Planet. Sci. Conf.* **26**, 1143 (1995); in preparation.
33. K. L. Tanaka, D. A. Senske, M. Price, R. L. Kirk, in (*2*), pp. 667–694.
34. S. A. Hauck II, R. J. Phillips, M. H. Price, *J. Geophys. Res.*, in press.
35. G. T. Jarvis and W. R. Peltier, in *Mantle Convection: Plate Tectonics and Global Dynamics*, W. R. Peltier, Ed. (Gordon & Breach, New York, 1989) pp. 479–593.
36. J. W. Head, *Lunar Planet. Sci.* **XXVI**, 573 (1995). Models that progressively flood crustal plateaus reveal characteristics typical of large tessera inliers, including arcuate marginal traces.
37. Coronae on Venus are ". . . any circular to elongate structure defined primarily by an annulus of concentric fractures and ridges." They occur most often in association with chasmata (rifts) [E. R. Stofan, V. E. Hamilton, D. M. Janes, S. E. Smrekar, in (*2*), pp. 931–965].
38. V. S. Solomatov, *Phys. Fluids* **7**, 266 (1995); G. Schubert, V. S. Solomatov, P. J. Tackley, D. L. Turcotte, in (*2*), pp.1245–1288; L.-N. Moresi and V. S. Solomatov, *Phys. Fluids* **7**, 2154 (1995); V. S. Solomatov and L.-N. Moresi, *J. Geophys. Res.* **101**, 4737 (1996).
39. L. Moresi and V. Solomatov, *Geophys. J. Inter.*, in press.
40. D. L. Turcotte, *J. Geophys. Res.* **100**, 16931 (1995).
41. G. G. Schaber *et al.*, *ibid.* **97**, 13257 (1992); R. G. Strom, G. G. Schaber, D. D. Dawson, *ibid.* **99**, 10899 (1994).
42. R. R. Herrick, *Geology* **22**, 703 (1994).
43. A. T. Basilevsky and J. W. Head, *Earth Moon Planets* **66**, 285 (1995).
44. Model calculations show that only modest increases (15%) of H_2O and SO_2 in the Venus atmosphere will drive the surface temperature to 1000 K [M. A. Bullock and D. H. Grinspoon, *J. Geophys. Res.* **101**, 7521 (1996)].
45. R. J. Phillips and M. C. Malin, in *Venus*, D. M. Hunten, L. Colin, T. M. Donahue, Eds. (Univ. of Arizona Press, Tucson, 1983), pp. 159–214.
46. D. J. Stevenson, T. Spohn, G. Schubert, *Icarus* **54**, 466 (1983).
47. The Nusselt number, *Nu*, is the ratio of conductive plus convective heat transport to conductive heat transport alone in a fluid system. The Rayleigh number, *Ra*, is the ratio of buoyancy forces to viscous forces in a fluid. These quantities are related through a power exponent β and a viscosity length scale p with power dependence α: $Nu \sim p^{\alpha} Ra^{\beta}$. The value of β is different for thin-lid and thick-lid convection (and $\alpha \equiv 0$ for thin-lid convection). Two coupled ordinary differential equations are integrated in time to obtain upper mantle (at base of lithospheric thermal boundary layer) and outermost core temperatures. Core energy balance includes the effects of solid inner core formation. Heat sources in the mantle are fractionated into a crust with time, and the heat flux out of the convecting mantle depends linearly on *Nu*.
48. The boundary layer bottom temperature is the outermost core temperature, and the top temperature is obtained by adiabatic extrapolation of the upper mantle solution temperature.
49. D. McKenzie, *J. Petrol.* **25**, 713 (1984); D. McKenzie and M. J. Bickle, *ibid.* **29**, 625 (1988).
50. The heat flow estimate in Table 1 is obtained from flexural modeling of a volcanic rise with a correction to the background value [R. J. Phillips *et al.*, in (*2*), pp. 1163–1204].
51. Parameter values are $f_p = 0.05$, $\Delta L_{plu} = 0.80$, $\Delta L_{upw} = 0.90$, $\Delta T_p = 0$ K, activation energy for creep divided by gas constant = 50,000 K, thermal diffusivity = 5×10^{-7} m^2 s^{-1}, β (thin lid) = 0.33, and β (thick lid) = 0.30.
52. If these calculations are carried forward in time, partial melting reaches a peak and then starts to slowly decrease due to the loss of heat-producing radiogenic parent isotopes in the mantle. This is also the reason for the slope prior to the switch.
53. N. H. Sleep [*J. Geophys. Res.* **95**, 6715 (1990)] presented a simple relationship between buoyancy flux in a plume (B in kg s^{-1}) and heat flow (H in W): where C_p is specific heat and α is volume coefficient of thermal expansion. Using this, the partial melt mass, M_{pm}, over a time interval, τ, can be related to heat flow from the core, q_c, by $M_{pm} = \alpha X 4\pi R_c^2 q_c \tau / C_p$, where X is the mass fraction of partial melt and R_c is core radius. This can be converted to volume of rock, assuming values for density and contraction. The subsequent mass is then divided by the root mass of a Tellus-Regio–sized crustal plateau (2×10^6 km^2, 1 km average height above its surroundings) using an isostatic assumption. This yields the number of Tellus-sized crustal plateaus generated by plumes over the interval τ.
54. This is obtained from an average melt volume fraction of 20% and an average core heat flux of 22 mW m^{-2} during the interval 1.7 Ga to 0.7 Ga.
55. R. H. Sibson, *J. Struct. Geol.* **7**, 751 (1985); M. P. Golombek and W. B. Banerdt, *Icarus* **68**, 252 (1986).
56. M. P. Golombek and W. B. Banerdt, *ibid.* **83**, 441 (1990).
57. This result is obtained by constructing a yield strength envelope [W. F. Brace and D. L. Kohlstedt, *J. Geophys. Res.* **85**, 6248 (1980)] using a dry diabase flow law [S. J. Mackwell, M. E. Zimmerman, D. L. Kohlstedt, D. S. Scherber, in *Proc. of the 35th U.S. Symposium on Rock Mechanics*, J. J. K. Daemen and R. A. Shultz, Eds. (A. A. Balkema, Rotterdam, 1995), pp. 207–214] and 10% strain in 0.1 My. The temperature profile used was for a cooling half-space model with a surface temperature of 740 or 1000 K and an initial temperature determined by mixing melt temperatures from the CMM with crustal temperatures from the CTM calculated with the appropriate surface temperature.
58. J. C. Jaeger and N. G. W. Cook, *Fundamentals of Rock Mechanics* (Chapman & Hall, New York, 1979). The transition depth for tensile to shear failure is dependent on the choice of tensile yield stress. We used a value of 10 MPa, which is within the range estimated for intact basalts [R. A. Schultz, *J. Geophys. Res.* **95**, 10883 (1993)].
59. C. G. Farnetani and M. A. Richards, *J. Geophys. Res.* **99**, 13813 (1994).

60. This work was supported by NASA's Planetary Geology and Geophysics programs under Grants NAGW-3024 to Washington University and NAGW-2915 to Southern Methodist University. D. Brown and S. Hauck provided helpful reviews of earlier drafts of this manuscript. We thank M. Zuber and two additional reviewers for comments. J. Goodge provided a review of the revised manuscript.